Crystal structure of the $Mg_{1-x}Al_xB_2$ superconductors near $x \approx 0.5$

Serena Margadonna,[1] Kosmas Prassides,[2,3] Ioannis Arvanitidis,[2] Michael Pissas,[3] Georgios Papavassiliou,[3] and Andrew N. Fitch[4]

[1]*Department of Chemistry, University of Cambridge, Cambridge CB2 1EW, United Kingdom*
[2]*School of Chemistry, Physics and Environmental Science, University of Sussex, Brighton BN1 9QJ, United Kingdom*
[3]*Institute of Materials Science, NCSR Demokritos, 153 10 Aghia Paraskevi, Athens, Greece*
[4]*European Synchrotron Radiation Facility, BP 220, 38042 Grenoble, France*

(Received 28 March 2002; published 9 July 2002)

Precise structural information on the $Mg_{1-x}Al_xB_2$ superconductors in the vicinity of $x \approx 0.5$ is derived from high-resolution synchrotron x-ray powder diffraction measurements. We find that a hexagonal superstructure, accompanied by doubling of the *c* axis, ordering of Mg and Al in alternating layers, and a shift of the *B* layers towards Al by ~ 0.12 Å, is formed. The unusually large width of the $(00\frac{1}{2})$ superlattice peak implies the presence of microstrain broadening, arising from anisotropic stacking of Al and Mg layers and/or structural modulations within the *ab* plane. The ordered phase survives only over a limited range of compositions away from the optimum $x = 0.5$ doping level.

DOI: 10.1103/PhysRevB.66.014518 PACS number(s): 74.62.−c, 61.10.Nz, 74.70.−b

The discovery of superconductivity in the binary boride, MgB_2 at the high temperature of 39 K (Ref. 1) has generated considerable interest because of the apparent simplicity of its chemical composition, crystal structure, and electronic properties. MgB_2 possesses a simple hexagonal structure (AlB_2-type, space group $P6/mmm$) comprising graphitic-type *B* layers interleaved with Mg layers.[2] Band structure calculations reveal that, while strong covalent *B*-*B* bonds are retained, Mg is fully ionized.[3] The charge carriers are situated in two essentially two-dimensional (2D) bands derived from the σ-bonding $p_{x,y}$ orbitals of boron, and in one electron and one hole band derived from the π-bonding p_z orbitals of boron. There is considerable experimental evidence [boron isotope effect,[4] scanning tunnelling experiments,[5] negative pressure coefficient of T_c (Ref. 6)] that a conventional phonon-mediated pairing mechanism can account for the superconducting properties of MgB_2, in which a key role is played by the 2D σ band of $p_{x,y}$ orbitals within the boron layers. Consistent with this, a small discontinuity only in the boron interlayer spacing was observed at T_c by precise structural measurements.[7]

Changes in carrier concentration and their influence on the electronic properties of the system can provide crucial tests for the mechanism of superconductivity and they have been investigated through chemical substitution between[8,9] or within[10] the boron layers. In all cases, the critical temperature of MgB_2 decreases at various rates for different substitutions. Among the various ternary compositions, the properties of the Al-doped series $Mg_{1-x}Al_xB_2$ are of particular interest and have been extensively studied both experimentally and theoretically. Electron doping through Al substitution leads to a decrease in T_c which can be rationalized by the filling of the electronic states by the additional electron donated by Al and the resulting decrease in the density of states at the Fermi level.[3] However, very importantly the rate of decrease of T_c, dT_c/dx sensitively depends on the doping level *x*.[8] T_c first decreases smoothly in the region $0 < x < 0.1$, then the transition becomes broader up to $x = 0.25$. For compositions with $0.25 < x < 0.4$, T_c drops more sharply and then superconductivity vanishes in the vicinity of $x = 0.6$.[11–13] These results imply a more complicated crystal structural and/or electronic response for the $Mg_{1-x}Al_xB_2$ series than that expected for solid solution and rigid band behavior. Indeed early x-ray diffraction measurements have revealed the presence of structural anomalies associated with a miscibility gap and multiphase behavior in the regions $0.1 < x < 0.25$ and $0.7 < x < 0.8$.[8] In addition, electron diffraction and transmission electron microscopy studies have provided direct evidence for the existence of a superstructure at $x \approx 0.5$ resulting from ordered arrangements of Al and Mg atoms both along the *c* axis[13,14] and in the *a*-*b* plane.[14]

In this paper, we report a structural determination of the $Mg_{1-x}Al_xB_2$ ($x = 0.45$, 0.5, 0.55) ternary superconductors by synchrotron x-ray powder diffraction at 16 and 298 K. A hexagonal superstructure, accompanied by the doubling of the *c* axis of the MgB_2 structure is observed, arising from ordering of Al and Mg in subsequent layers. Formation of the superstructure is optimal for $Mg_{0.5}Al_{0.5}B_2$ but survives small deviations ($\approx 10\%$) from the $x = 0.5$ composition.

Powder samples with nominal composition $Mg_{1-x}Al_xB_2$ with $x = 0.4$, 0.45, 0.5, and 0.55 were prepared by a slightly modified method of Ref. 15. We have observed after repeated trials that Mg excess is not necessary for the preparation of $Mg_{1-x}Al_xB_2$ samples with $0.3 \leqslant x \leqslant 1$. Consequently, the present samples were prepared by mixing stoichiometric quantities of Al, Mg, and amorphous B and heating for 24 h at temperatures between 800 and 870 °C, depending on the value of *x*. SQUID measurements were performed on 50-mg samples in the temperature range 1.8–50 K with a Quantum Design SQUID magnetometer (MPMS5). High-resolution synchrotron x-ray diffraction experiments were carried out on the BM16 beamline at the European Synchrotron Radiation Facility (ESRF), France. The samples were sealed in 1.0-mm diameter glass capillaries and diffraction profiles ($\lambda = 0.85023$ Å) were collected at 16 K (and for $x = 0.5$ also at ambient temperature) in continuous scanning mode using

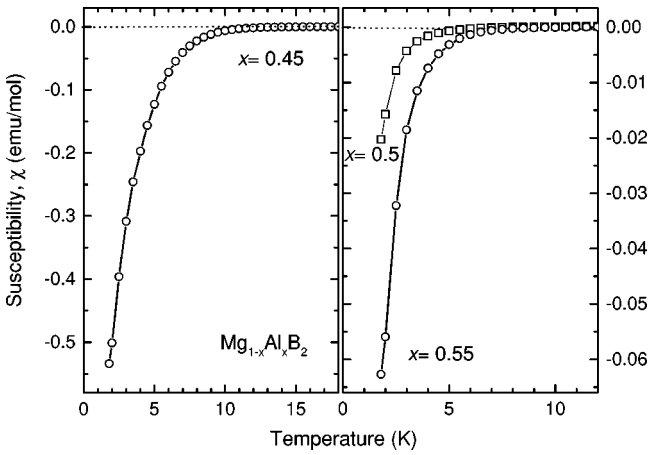

FIG. 1. Temperature dependence of the magnetic susceptibilities of $Mg_{1-x}Al_xB_2$ ($x=0.45$, 0.5, and 0.55) measured under ZFC conditions in a field of 10 Oe.

nine Ge(111) analyzer crystals. The capillaries were continuously spun during data acquisition. The data were rebinned in the 2θ range $1°-80°$ to a step of 0.01° and refined using the GSAS suite of Rietveld analysis programs. The peak shape of the diffraction lines was modeled by a convolution of a pseudo-Voigt function and an asymmetry function, which is related to the instrumental axial divergence.[16] In addition, in order to account for anisotropic peak broadening of different classes of (hkl) reflections evident in the high-resolution diffraction profiles, the Gaussian and Lorentzian portions of the peak shape function ascribed to microstrain broadening (σ_s^2 and γ_s) were described by the semiempirical Stephens formalism.[17] In this model, the width of each reflection can be expressed in terms of moments of a multidimensional distribution of lattice metric parameters and can be related to distributions of elastic strains caused by defects or dislocations.

Figure 1 shows the results of the magnetic measurements at 10 Oe (ZFC conditions) for the $Mg_{1-x}Al_xB_2$ compositions with $x=0.45$, 0.5, and 0.55. Diamagnetic shielding is evident at low temperature in all three samples. The transition temperatures T_c, defined by the intersection of line extrapolations below and above T_c, are 6, 3, and 4 K for $x=0.45$, 0.5, and 0.55, respectively. Although the shielding fractions at 2 K are small, the transitions are considerably sharper than those reported for phase separated samples,[8] implying that superconductivity is of bulk nature and does not arise from sample inhomogeneities and composition fluctuations.

Inspection of the synchrotron x-ray diffraction profile of $Mg_{0.5}Al_{0.5}B_2$ at 16 K shows that all reflections can be assigned either to a hexagonal cell (space group $P6/mmm$, AlB_2 type) with lattice constants $a\approx3.045$ Å and $c\approx3.506$ Å or to a small fraction ($<1\%$) of MgO impurity. However, an additional weak peak not attributable to an impurity phase is clearly visible at $2\theta=7.26°$ (Fig. 2). This extra reflection whose intensity is $\sim26\%$ of the weak (001) reflection indexes as $(00\frac{1}{2})$ on the hexagonal unit cell and provides the unambiguous signature of the formation of a superstructure whose unit cell is exactly doubled along the

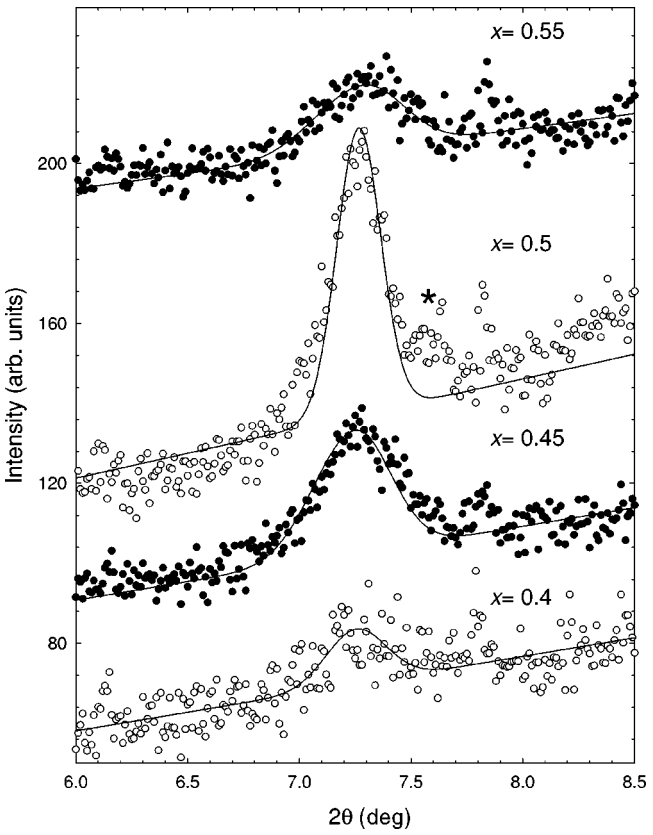

FIG. 2. Synchrotron x-ray powder diffraction profiles of $Mg_{1-x}Al_xB_2$ ($x=0.4$, 0.45, 0.5, and 0.55) at 16 K in the vicinity of the $(00\frac{1}{2})$ superlattice reflection. The solid lines are guides to the eye.

c axis. No other prominent peaks that could arise from the formation of the superstructure are observed under the present experimental conditions. The observed doubling of the *c* axis allows ordering of Al and Mg in subsequent layers while maintaining the gross features of the original AlB_2-type structure. The simplest Al/Mg ordering motif consistent with the observed superreflection corresponds to an alternation of Al and Mg along the *c* axis (space group $P6/mmm$), as suggested by TEM investigations in Ref. 13. Rietveld refinements using this model proceeded smoothly with Mg and Al placed in the $1a(0,0,\frac{1}{2})$ and $1b(0,0,0)$ positions, respectively, and the B atoms located in the $4h$ $(\frac{1}{3},\frac{2}{3},z;z\approx\frac{1}{4})$ positions. The refined lattice parameters of $Mg_{0.5}Al_{0.5}B_2$ at 16 K are $a=3.04436(2)$ Å and $c=6.71248(10)$ Å, while the Mg and Al content refined as 0.52(3) and 0.48(3), respectively, in agreement with the nominal composition. In addition to Al/Mg ordering, the present structural model allows for unequal separation between neighboring MgB_2 and AlB_2 slabs as the B atoms have the freedom to relax along the *c* direction ($z\neq\frac{1}{4}$), while the strictly flat boron sheets of the original AlB_2-type structure are maintained (Fig. 3). In $Mg_{0.5}Al_{0.5}B_2$, the B position refines to $[\frac{1}{3},\frac{2}{3},0.2413(3)]$, corresponding to Mg-B and Al-B distances of 2.471(1) and 2.390(1) Å, respectively.

In the course of the Rietveld refinements, it was evident

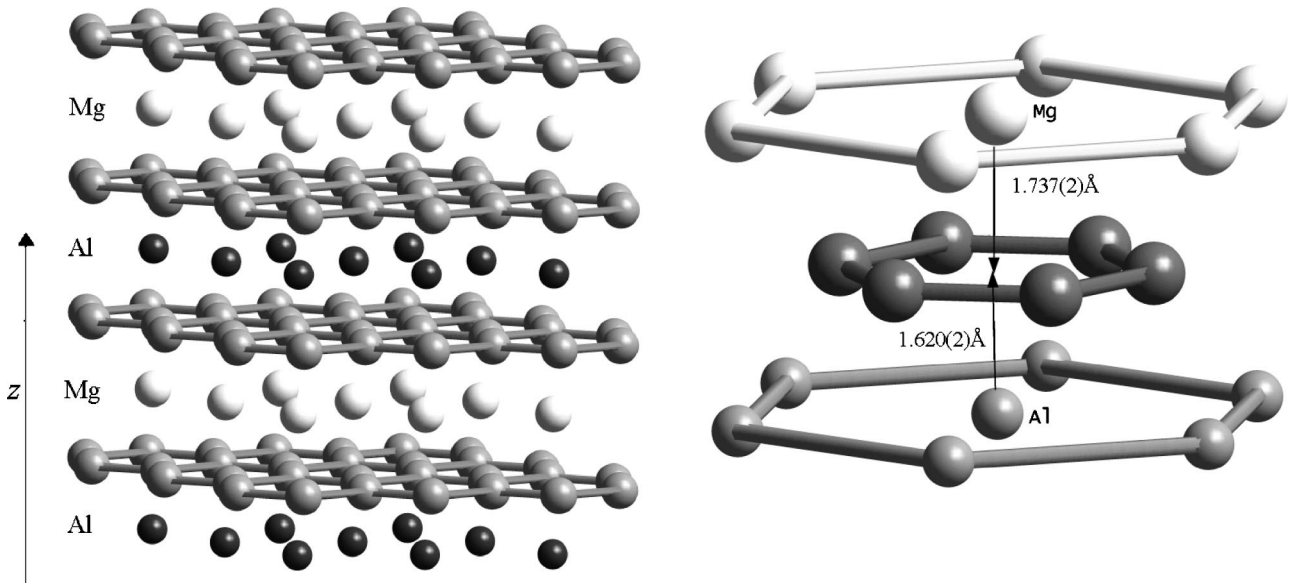

FIG. 3. Structural model of the $Mg_{0.5}Al_{0.5}B_2$ superstructure.

that the widths of the $(00l)$ reflections were invariably larger than those of the $(hk0)$ reflections, providing the signature of strong anisotropic strain broadening effects. These microstructural effects were modeled with the formalism developed by Stephens.[17] For this model, the obtained microstrain broadening contribution to the width of the (001) reflection is $\sim 1.3\%$, almost twice as large as that of the (200) peak. This could be related to increased strains along the c axis due to the presence of defects and stacking faults associated with the Al and Mg layers. Moreover, the microstrain contribution to the width of the $(00\frac{1}{2})$ superlattice peak is even higher $(\sim 4.1\%)$ implying an anisotropic distribution along the c axis of alternating ordered Al and Mg layers. Figure 4 displays the final refinement of the synchrotron x-ray diffraction profile of $Mg_{0.5}Al_{0.5}B_2$ at 16 K, while the results of the analysis are summarized in Table I.

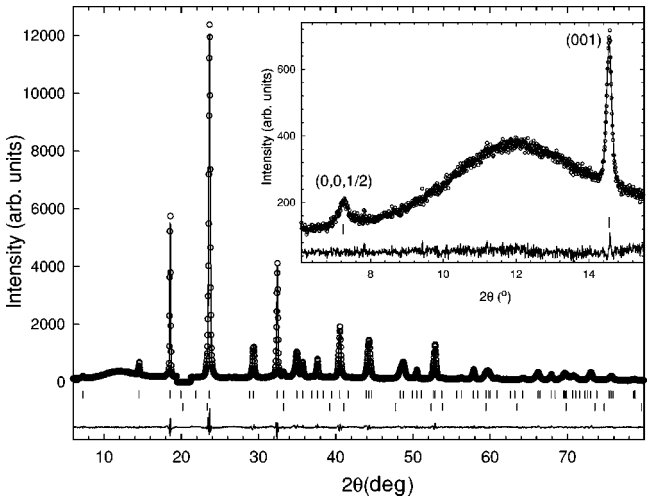

FIG. 4. Final observed (points) and calculated (solid line) synchrotron x-ray powder diffraction profiles for $Mg_{0.5}Al_{0.5}B_2$ at 16 K in the range 6° to 80° ($\lambda = 0.85023$ Å). The lower panel shows the difference profiles and the ticks mark the positions of the Bragg reflections of $Mg_{0.5}Al_{0.5}B_2$ (upper) and MgO ($<1\%$, lower). Inset. Rietveld fit in the range 6° to 15.6°.

Despite the excellent quality of the Rietveld refinement of the synchrotron x-ray diffraction profile of $Mg_{0.5}Al_{0.5}B_2$ using the Al/Mg ordering model described above, alternative models of ordering were also considered. An attractive possibility consistent with the observed doubling of the hexagonal c axis involves ordering of both Al and Mg on the same layer with each atom surrounded by as many atoms of the other kind as possible. However, the resulting crystal symmetry is $P6_3/mmc$ and the $(00\frac{1}{2})$ reflection will be extinct, clearly necessitating ordering of Al and Mg atoms in alternating layers. Finally, we considered the possibility that ordering of Mg and Al is accompanied by distortion of the B layers. The appropriate unit cell in this case is primitive orthorhombic with lattice constants $a \approx a_h$, $b \approx b_h\sqrt{3}$, and $c = 2c_h$. Rietveld refinements of the diffraction data using such models did proceed to convergence and improved quality of fit but the paucity of observed superreflections did not allow unambiguous conclusions concerning the existence of an orthorhombic distortion of the original hexagonal unit cell.

TABLE I. Refined parameters for $Mg_{0.5}Al_{0.5}B_2$ obtained from Rietveld refinement of synchrotron x-ray powder diffraction data at 16 K (space group $P6/mmm$; hexagonal cell constants: $a = 3.04436(2)$ Å, $c = 6.71248(10)$ Å; reliability factors $R_{wp} = 5.4\%$, $R_{exp} = 4.0\%$). The lattice constants at 298 K are $a = 3.04705(2)$ Å, $c = 6.72409(12)$ Å and the reliability factors $R_{wp} = 6.1\%$, $R_{exp} = 5.1\%$.

Atom	Site	x/a	y/a	z/c	B(Å^2)	occupancy
Mg	$1a$	0	0	$\frac{1}{2}$	0.17(1)	1.04(6)
Al	$1b$	0	0	0	0.17(1)	0.96(6)
B	$4h$	$\frac{1}{3}$	$\frac{2}{3}$	0.2413(3)	0.93(3)	1.1(2)

TABLE II. Selected bond distances (Å) in $Mg_{1-x}Al_xB_2$ ($x=0.4,\ 0.45,\ 0.5,\ 0.55$) at 16 K.

x	Mg-B	Al-B	(Mg/Al)-B	B-B
0.4			2.44157(2)	1.76365(1)
0.45	2.438(2)	2.433(2)		1.76085(1)
0.5	2.471(1)	2.390(1)		1.75766(1)
0.55	2.442(2)	2.410(2)		1.75692(1)

A synchrotron x-ray diffraction profile of $Mg_{0.5}Al_{0.5}B_2$ was also collected at 298 K. The $(00\frac{1}{2})$ superlattice peak is again present implying the absence of a phase change with increasing temperature. Rietveld refinement with the $P6/mmm$ superstructure model proceeded smoothly (Table I), leading to lattice constants of $a=3.04705(2)$ Å and $c=6.72409(12)$ Å and anisotropic expansion between 16 and 298 K of 0.088(1) and 0.173(3) % along the a and c axis, respectively.

Synchrotron x-ray diffraction profiles were also collected at 16 K for the $Mg_{0.55}Al_{0.45}B_2$ and $Mg_{0.45}Al_{0.55}B_2$ compositions. In both cases, the peak at $2\theta\approx 7.26°$ which provides the signature of Mg/Al ordering and superstructure formation is present but with decreased intensity [≈ 11 and 18 % of the corresponding (001) reflections, respectively] and increased width when compared to that in $Mg_{0.5}Al_{0.5}B_2$ (Fig. 2). The two diffraction profiles were refined using the same structural model discussed above. In the case of $Mg_{0.45}Al_{0.55}B_2$, the excess Mg (5%) present was disordered in the Al layers, while for $Mg_{0.45}Al_{0.55}B_2$, the excess Al (5%) in the Mg layers. The Rietveld refinements proceeded smoothly and the refined values of the lattice constants are $a=3.04318(3)$ Å, $c=6.69127(12)$ Å, and $a=3.04988(2)$ Å, $c=6.73190(11)$ Å for $Mg_{0.45}Al_{0.55}B_2$ and $Mg_{0.55}Al_{0.45}B_2$, respectively (Table II). The Mg and Al stoichiometries refined to 0.47(3) and 0.54(3) for the sample with nominal composition $Mg_{0.45}Al_{0.55}B_2$ and to 0.56(4) and 0.45(4) for $Mg_{0.55}Al_{0.45}B_2$.

A perspective view of the hexagonal superstructure of $Mg_{0.5}Al_{0.5}B_2$ is shown in Fig. 3. Compared to the unit cell of MgB_2, the present structure arises from ordering of the Mg^{2+} and Al^{3+} ions, leading to doubling of the unit cell along the c axis. Both crystallographically distinct Mg^{2+} and Al^{3+} ions present in the unit cell have identical coordination environments, namely, they lie directly above the centers of two B hexagons of adjacent B layers. Consistent with the higher ionic charge and smaller ionic radius (0.675 Å) of Al^{3+} compared to Mg^{2+} (0.860 Å), the Al-B bond distances are smaller than the Mg-B ones, 2.390(1) Å and 2.471(1) Å, respectively, at 16 K. This leads to Al-B and Mg-B layer separations along the c direction of 1.620(2) Å and 1.737(2) Å, respectively, and reflects a displacement of the B layers of ~ 0.12 Å towards each Al layer. As we deviate from the $x=0.5$ ternary towards Mg or Al rich compositions, the difference between the Al-B and Mg-B layer separations rapidly decreases (only ~ 0.01 and 0.05 Å, respectively, for $x=0.45$ and 0.55, Table II). The ordered superstructure is essentially destroyed for $Mg_{0.6}Al_{0.4}B_2$, as the $(00\frac{1}{2})$ superlattice peak has now collapsed into the background (Fig. 2), while further it is unambiguously absent in compositions with even smaller Al doping levels. On the other hand, the in-plane B-B bond lengths decrease monotonically with increasing Al content across the stability boundary of the superstructure [from 1.76365(1) Å in $Mg_{0.6}Al_{0.4}B_2$ to 1.75692(1) Å in $Mg_{0.45}Al_{0.55}B_2$] in agreement with the strengthening of the in-plane σ bonds.

The superstructure derived in this work is identical to that proposed by earlier TEM measurements[13] and is energetically preferred, according to recent theoretical calculations.[18] In addition, a more complicated Mg/Al ordering scheme, involving both ordering along the c axis and a sinusoidal modulation component, q in the hexagonal ab plane was observed in the HREM work of Zandbergen *et al.*[14] The signature of the in-plane structural modulation came from the splitting of the observed superreflections which yielded diffraction rings. In the present powder x-ray diffraction experiments, no such clear splittings are observed. However, we first note that the observed $(00\frac{1}{2})$ superreflection is unusually broad (Fig. 2) and the large microstrain broadening (*vide supra*) required to account for its width may be precisely associated with such ordered distributions of the Mg and Al atoms within the hexagonal planes. In addition, there is a shoulder on the high angle side of the $(00\frac{1}{2})$ peak at $2\theta\approx 7.5°$ (marked with an asterisk in Fig. 2) which indexes as $(q_1, q_2, \frac{1}{2})$ with $(q_1^2+q_2^2)^{1/2}\approx 0.12$, tantalizingly close to the incommensurate in-plane modulation vector $q\approx 0.1$ in Ref. 14.

The origin of the observed superstructure is of particular importance and may have consequences for the understanding of superconductivity in these systems. One possibility is that it is associated with an electronic instability near the 50% doping level.[14] This is consistent with the extremely narrow stability range of the superstructure and its sensitivity to small compositional changes. In addition, T_c is somewhat suppressed at $x\approx 0.5$ where the superstructure formation is optimal but superconductivity does not completely disappear, as it would be expected from the opening of a gap at the Fermi surface. However, a small off-stoichiometry effect being responsible for the observed diamagnetic shielding cannot be excluded, despite the high quality of the present $Mg_{0.5}Al_{0.5}B_2$ sample precluding large compositional fluctuations. Another possibility is that it is associated with a structural instability arising from the size mismatch between Al and Mg. The Al-B and Mg-B bond distances are 2.375 and 2.501 Å in the AlB_2 and MgB_2 end members, respectively. Doping of AlB_2 with Mg or MgB_2 with Al has only a small effect on the in-plane lattice constants but affects principally the interlayer separations. In both cases, increased doping is accompanied by the appearance of phase separation at certain critical levels.[8,11,13] The coexisting phases differ mainly in their c-lattice constants and contain different concentrations of Mg and Al in the metal layers. In the vicinity of $x\approx 0.5$, the size mismatch effect is maximal and complete ordering of Mg and Al becomes energetically favorable. The observed Al-B and Mg-B bond distances of 2.390(1) and 2.471(1) Å in the $Mg_{0.5}Al_{0.5}B_2$ superstructure are compa-

rable to those encountered for the $x \approx 0.8$ and 0.2 compositions, respectively, near the Al- and Mg-rich critical concentrations for the two-phase separation onsets in the $Mg_{1-x}Al_xB_2$ series.

In conclusion, a hexagonal superstructure is obtained in $Mg_{1-x}Al_xB_2$ for a small range of Al and Mg concentrations near $x \approx 0.5$. The principal component of the structural modulation of the parent MgB_2 structure is along the *c*-axis, while evidence exists for anisotropic distributions of alternating Mg/Al planes in the *c* direction or ordered Mg/Al distributions within the hexagonal planes. Size mismatch and electronic effects were considered as possible origins of the observed behavior.

We thank the ESRF for provision of synchrotron x-ray beamtime. S.M. thanks Jesus College, Cambridge for financial support. The research has been supported by a Marie Curie Fellowship of the EU program ''Improving the Human Research Potential'' under contract number HPMF-CT-2001-01436.

[1] J. Nagamatsu, N. Nakagawa, T. Muranaka, Y. Zenitani, and J. Akimitsu, Nature (London) **410**, 63 (2001).
[2] M.E. Jones and R.E. March, J. Am. Chem. Soc. **76**, 1434 (1954).
[3] J.M. An and W.E. Pickett, Phys. Rev. Lett. **86**, 4366 (2001); J. Kortus, I.I. Mazin, K.D. Belashchenko, V.P. Antropov, and L.L. Boyer, *ibid.* **86**, 4656 (2001).
[4] S.L. Bud'ko, G. Lapertot, C. Petrovic, C.E. Cunningham, N. Anderson, and P.C. Canfield, Phys. Rev. Lett. **86**, 1877 (2001); D.G. Hinks, H. Claus, and J.D. Jorgensen, Nature (London) **411**, 457 (2001).
[5] G. Karapetrov, M. Iavarone, W.K. Kwok, G.W. Crabtree, and D.G. Hinks, Phys. Rev. Lett. **86**, 4374 (2001).
[6] B. Lorenz, R.L. Meng, and C.W. Chu, Phys. Rev. B **64**, 12 507 (2001); E. Saito, T. Takenobu, T. Ito, Y. Iwasa, K. Prassides, and T. Arima, J. Phys.: Condens. Matter **13**, L267 (2001).
[7] S. Margadonna, T. Muranaka, K. Prassides, I. Maurin, K. Brigatti, R.M. Ibberson, M. Arai, M. Takata, and J. Akimitsu, J. Phys.: Condens. Matter **13**, L795 (2001).
[8] J.S. Slusky, N. Rogado, K.A. Regan, M.A. Hayward, P. Khalifah, T. He, K. Inumaru, S.M. Loureiro, M.K. Haas, H.W. Zandbergen, and R.J. Cava, Nature (London) **410**, 343 (2001).
[9] Y.G. Zao, X.P. Zhang, P.T. Qiao, H.T. Zhang, S.L. Jian, B.S. Cao, M.H. Zhu, Z.H. Han, X.L. Wang, and B.L. Gu, Physica C **361**, 91 (2001).
[10] T. Takenobu, T. Ito, D.H. Chi, K. Prassides, and Y. Iwasa, Phys. Rev. B **64**, 134513 (2001); I. Maurin, S. Margadonna, K. Prassides, T. Takenobu, T. Ito, D.H. Chi, Y. Iwasa, and A. Pitch, Physica B (to be published).
[11] P. Postorino, A. Congeduti, P. Dore, A. Nucara, A. Bianconi, D. Di Castro, S. De Negri, and A. Saccone, Phys. Rev. B **65**, 020507 (2001).
[12] B. Renker, K.B. Bohnen, R. Heid, D. Ernst, H. Schober, M. Koza, P. Adelmann, P. Schweiss, and T. Wolf, Phys. Rev. Lett. **88**, 067001 (2002).
[13] J.Q. Li, L. Li, F.M. Liu, C. Dong, J.Y. Xiang, and Z.X. Zhao, Phys. Rev. B **65**, 132505 (2002).
[14] H.W. Zandbergen, M.Y. Wu, H. Jiang, M.A. Hayward, M.K. Haas, and R.J. Cava, Physica C **366**, 221 (2002).
[15] M. Pissas, E. Moraitakis, D. Stamopoulos, G. Papavassiliou, V. Psycharis, and S. Koutandos, J. Supercond. **14**, 615 (2001).
[16] P.E. Thompson, D.E. Cox, and J.B. Hasting, J. Appl. Crystallogr. **20**, 79 (1987); L.W. Finger, D.E. Cox, and A.P. Jephcoat, *ibid.* **27**, 892 (1994).
[17] P.W. Stephens, J. Appl. Crystallogr. **32**, 281 (1999).
[18] S.V. Barabash and D. Stroud, cond-mat/0111392 (unpublished).